Investigation of a Compound Helicopter Flying the Depart and Abort Mission Task Element

Kevin Ferguson
Kevin.Ferguson@selex-es.com
Research Assistant
University of Glasgow
Glasgow, United Kingdom

Douglas Thomson
Douglas.Thomson@glasgow.ac.uk
Senior Lecturer
University of Glasgow
Glasgow, United Kingdom

Dave Anderson
Dave.Anderson@glasgow.ac.uk
Senior Lecturer
University of Glasgow
Glasgow, United Kingdom

ABSTRACT

The next generation of rotorcraft will have to satisfy the appropriate handling qualities requirements before entering service. Many of these vehicles will operate at significantly greater speeds than the conventional helicopter and will therefore have different capabilities than current helicopters. Due to the different capabilities of the compound helicopter, it is possible that new Mission Task Elements (MTEs) need to be developed to assess the handling qualities of this type of helicopter. It is also possible that existing MTEs may be suitable without modification. Overall, it seems necessary to review the US Army's current handling qualities specification, ADS-33, and determine the suitability of the current MTEs for compound vehicles. The broad aim of the paper is to assess the performance of compound helicopter during manoeuvring flight. More specifically, a simulation study of a compound helicopter flying the Depart and Abort ADS-33 Mission Task Element. There are two objectives: firstly the capabilities of the compound vehicle is compared with those of a conventional helicopter, and secondly, the suitability of the current Depart and Abort MTE, for compound vehicles, is assessed. The results of the research study highlight the capability of compound helicopters in low speed acceleration manoeuvres. These results can be used to redefine low speed acceleration manoeuvres in the new update to the ADS-33 specification. The results also indicate some information about the potential design issues with the compound helicopter.

NOMENCLATURE

Main Nomenclature List

α_{bl}	blade angle of attack (rad)
χ	track angle (rad)
δ_c	collective lever or lateral stick position (%)
δ_s	longitudinal stick position (%)
δ_{tr}	foot pedal position (%)
ε	blade angle of attack where the maximum lift-to-drag ratio occurs
γ	glideslope angle (rad)

Presented at the AHS Rotorcraft Handling Qualities, Huntsville, Alabama, February 22–23, 2017.

γ_{rot}	main rotor Lock number
ρ	air density (kg/m^3)
Γ	tail-rotor cant angle (deg)
σ	main rotor solidity
θ_0	main rotor collective angle (rad)
θ_{0tr}	tail-rotor collective angle (rad)
θ_{1s}	main rotor longitudinal cyclic angle (rad)
θ_{1c}	main rotor lateral cyclic angle (rad)
θ_{prop}	Cheyenne propeller pitch angle (rad)
θ_{tw}	blade twist (rad)
e	Oswald efficiency factor
f_e	equivalent flat plate area (m^2)
m	aircraft mass (kg)
$\mathbf{u}$	control vector (rad)
$\mathbf{y}_{des}$	desired aircraft trajectory (various units)
x_e, y_e, z_e	aircraft position in Earth axes (m)
AR	aspect ratio
Ω	main rotor rotational speed (rad/s)
Φ, Θ, Ψ	Euler angles (rad)
C_D, C_L	drag and lift coefficient
C_T	thrust coefficient
D	drag (N)
L_w	wing lift (N)
$I_{xx}, I_{yy}, I_{zz}, I_{xz}$	moments of inertia (kg.m^2)
P	power (kW)
R	main rotor radius (m)
S	wing area (m^2)
T	thrust (N)
V_f	airspeed (kt or m/s)
W	aircraft weight (N)
X	propeller thrust at trim (N)

Subscripts

prof	profile drag
prod	produced
prop	propeller
ind	induced drag
req	required
fin	fin
flat	flat plate
fus	fuselage
rot	rotor
tr	tail-rotor
tw	twist
w	wing

INTRODUCTION

The compound helicopter is again being explored as it can potentially satisfy the emerging requirements for the next generation of rotorcraft. The US Army started their Joint Multi-Role (JMR) programme in 2014, which aims to

replace their existing fleet with helicopters with greater speed and range capability (Ref. **?**). As a result, some helicopter manufacturers are investigating the compound helicopter design, as it can potentially satisfy the requirements of the JMR programme. For example, Sikorsky have recently concluded their testing of the Sikorsky X2, with the flight tests indicating promising results. The testing of the Sikorsky X2 programme was so successful that Sikorsky have taken this concept to the next level by developing the Sikorsky S-97 Raider®. The Sikorsky S-97 Raider is envisioned to be a multi-role aircraft which can complete various military missions including close-air support and armed reconnaissance. In addition, Airbus Helicopters have flight tested their prototype - the Airbus Helicopters X^3. It is clear that some helicopter manufacturers are investigating the compound helicopter design, as it can potentially satisfy the requirements of the JMR programme. It is also clear that compound helicopter designs will operate at significantly greater speeds than the conventional helicopter and will therefore have different capabilities than current helicopters. Due to the different capabilities of the compound helicopter, it is possible that new Mission Task Elements (MTEs) need to be developed to assess the handling qualities of this type of helicopter. It is also possible that existing MTEs may be suitable without modification. Overall, it seems necessary to review the US Army's current handling qualities specification, ADS-33, and determine the suitability of the current MTEs for compound vehicles.

The broad aim of the collaboration between the University of Glasgow and the US Army's Research, Development and Engineering Command (RDECOM) is to assess the performance of compound helicopters during manoeuvring flight. More precisely, this study focuses on the Depart and Abort MTE and examines how a compound helicopter would fly this particular test manoeuvre. There are two main objectives from the study. The first objective is assess the capabilities of the compound vehicle and compare these capabilities with a conventional helicopter. The second objective is to determine the suitability of the current Depart and Abort MTE for compound vehicles.

This research aim is achieved by using the flight dynamics tool of inverse simulation. Inverse simulation reverses the process of conventional simulation. With conventional simulation, a control input is applied to the mathematical model and a response is observed. Inverse simulation does the opposite and the manoeuvre of interest becomes the input to the simulation, and the vehicle response and pilot control activity required to fly it are computed. One of the benefits of inverse simulation is that it does not require detailed knowledge of the underlying model and is thus extremely effective for investigating performance and control strategies. To use the inverse simulation algorithm successfully requires three key elements: a mathematical model, a manoeuvre model and the inverse simulation algorithm itself. Each of these elements are discussed in the subsequent sections.

MATHEMATICAL MODELLING

For the majority of the study, the mathematical model used is a 6 degrees of freedom nonlinear model with a disc representation of the main rotor. This is a well established formulation (Ref. **?**), which provides valid and usable results over a wide range of flight conditions. This model is referred to as the "level 1" model, which is consistent with the modelling hierarchy as defined by Padfield (Ref. **?**). Comprehensive descriptions of this model can be found in the literature (Refs. **?**, **?**, **?**), therefore only a short description is given here. The level 1 main rotor model ignores the pitching and lagging degrees of freedom, therefore assuming that the flap dynamics have the most influence in terms of the helicopter's flight dynamic characteristics. The flapping dynamics are assumed to be quasi-steady, a common assumption in main rotor modelling, therefore permitting a multi-blade representation of the main rotor. The main rotor is assumed to be centrally hinged with stiffness in flap and with the main rotor chord assumed to be constant. Furthermore, the model also features a steady momentum inflow and a rotor-speed governor model. One of the short comings of this type of model is that it is unable to model nonlinear aerodynamics. This limitation becomes important in high speed flight as compressibility effects and blade stalling need to be modelled to successfully capture the behaviour of the helicopter's main rotor (Ref. **?**). To accommodate this modelling deficiency a new helicopter main rotor model was developed, which is referred to as the "level 2" model. The main difference between the two models is that nonlinear aerodynamics are modelled in the level 2 model. As a result, the level 2 model is able to model compressibility effects, reverse flow and blade stalling. It should be stressed that this is not a modelling study, therefore only a limited amount of time was dedicated to developing this level 2 model.

Fig. 1. The UH-60 "Blackhawk" Helicopter

Consequently, the majority of the results presented in this study were generated using the level 1 model. The validity of these types of models are discussed further in the report.

UH-60A Helicopter Model

The modelling strategy used in this study is to use an established mathematical model of a conventional helicopter, and then convert this model to represent a compound helicopter configuration. One of the first tasks in the study is to configure the mathematical model to represent a conventional helicopter. The conventional helicopter selected is the UH-60A, as shown in Figure **??**. The UH-60A helicopter is a utility transport helicopter developed by Sikorsky, which performs various missions such as aeromedical evacuations and troop assaults. It is a twin-engined medium sized helicopter, designed for a gross weight of 7200 kg, and its main design parameters are shown in Table **??**. The main rotor of the vehicle features four articulated rotor blades coupled with hydraulic lag dampers. The helicopter also features a canted tail-rotor which provides additional lift in the hover and extends the centre of gravity range of the aircraft (Ref. **?**). Another key design feature is the moveable tailplane, with the incidence of the tailplane being a function of airspeed, collective lever position, pitch rate and lateral acceleration. The UH-60A configuration is used for a starting point in this study for two primary reasons. Firstly, the data-set is in the public domain (Refs. **?**, **?**) thereby allowing dissemination of results. Secondly, the UH-60A helicopter falls into the utility helicopter category, which is the type of helicopter the Joint Multi Role (JMR) programme will be developing.

Compound Helicopter Configuration

The next step is to take the conventional helicopter, Figure **??**, and convert it to model a compound configuration. The compound configuration examined is a similar configuration to the Lockheed Cheyenne helicopter. This configuration features a wing and a pusher propeller mounted at the tail of the airframe. A sketch of this compound helicopter configuration is shown in Figure **??**. The end result is two helicopter configurations: a conventional helicopter and a compound helicopter configuration.

Design Considerations

Wing Design The compound helicopter configuration have been introduced. The addition of wings and a pusher propeller to the helicopter, see Figure **??**, means that some preliminary design issues need to be taken into account. The first task is to size the wing. Orchard and Newman investigated the design of compound helicopter (Ref. **?**). Their study suggests that a medium size wing should be used to provide a compromise between the beneficial effect of offloading the rotor at high speeds and the adverse effect of creating an aerodynamic download at low speeds (Ref. **?**). Their study also highlights the importance of the wing design to the vehicle, suggesting that an

Design Parameter	Value
m	7200 kg
R	8.18 m
Ω	27 rad/s
σ	0.08210
γ_{rot}	8.19
θ_{tw}	-18 deg (nonlinear)
I_{xx}	6290 kg.m^2
I_{yy}	51991 kg.m^2
I_{zz}	49895 kg.m^2
I_{xz}	2541 kg.m^2
R_{tr}	1.68 m
Ω_{tr}	125 rad/s
σ_{tr}	0.1875
$\theta_{tr\,tw}$	-18 deg
Γ	20 deg

Table 1. Important Design Parameters of the UH-60A Helicopter (Ref. ?)

aspect ratio of 6 would be appropriate so that the wing does not extend into a region where the the main rotor's tip vortex would adversely affect the wing's performance (Ref. **?**). All of these issues should be taken into account when sizing the wing. Another important study by Yeo and Johnson (Ref. **?**) concluded that the optimum cruise condition occurs when the wing carries 91-92% of the aircraft weight. It also makes sense to design the wing so that it operates at its maximum lift-to-drag ratio at cruise. The assumed cruise condition of the compound helicopter is 210kt at an altitude of 1800m. These two values have been loosely based on the requirements of the JMR programme (Ref. **?**). The estimated wing area is found by using the following Equation

$$S = \frac{2L_w}{\rho V^2 C_L} \tag{1}$$

where L_w is the lifting force of the wing (assumed to be 91% of the aircraft's weight), and the other terms retain their usual meaning. The lift coefficient corresponds to the condition where the wing's aerofoil lift-to-drag ratio is at its highest. For the compound helicopter the NACA-65A-618 aerofoil is used due to its low profile drag at trim, its relatively high lift coefficient, gentle stall characteristics and its high lift curve slope (Ref. **?**). For this particular aerofoil the maximum lift-to-drag ratio occurs when $C_L = 0.6$. Using this lift coefficient and the appropriate cruise flight conditions then the wing area, S of the compound helicopter is calculated to be 17.6 m^2. This choice of wing area is a design compromise between minimising the hover penalty of the wing whilst having the ability to offload the main rotor in high speed flight.

Another design decision is the selection of the aspect ratio. The choice of aspect ratio was based on historical data of winged helicopters which have previously flown, which include the NH-3A and SA341 Gazelle helicopters (Refs. **?**,**?**), leading to the design choice of 6. This choice is also supported by Orchard and Newman (Ref. **?**), as previously stated. The taper ratio of each wing is selected to be 0.5, in an attempt to reduce the amount of induced drag (Ref. **?**).

Main Rotational Speed Variation Due to the expansion of the flight envelope, it is necessary to reduce the rotational speed of the compound helicopter's main rotor in high speed flight (Ref. **?**). This is required to avoid adverse compressibility effects in forward flight. This design feature is incorporated on all modern compound helicopters. In this study, the main rotor planform of each helicopter configuration is the same. The only difference between the main rotor design of the conventional helicopter when compared to the compound helicopter is the rotational speed

(a) Baseline Helicopter

(b) Cheyenne Compound Helicopter

Fig. 2. Sketches of the two Helicopter Configurations

in forward flight. Figure **??** shows how the rotational speed of the compound helicopter's main rotor varies with airspeed. Note that the rotorspeed of the UH-60A helicopter is a constant value of 27 rad/s throughout the flight envelope. In relation to the compound helicopter, at 130 kt the main rotor's speed is gradually lowered to avoid the assumed drag divergence Mach number. The drag divergence Mach number is the Mach number where the drag coefficient rises significantly (Ref. **?**). This is commonly defined as the Mach number were the drag coefficient rises at a rate of 0.1 per unit Mach number (Ref. **?**). Experimental results from various studies confirm that the drag divergence Mach number for typical helicopter aerofoils ranges between 0.85-0.92 (Refs. **?**, **?**). The value of 0.87 is selected for this study. At 210 kt, the main rotor is slowed to 81% (see Figure **??**), thereby avoiding an advancing tip Mach number of 0.87. The design decision here is to keep the rotorspeed as high as possible, without compressibility effects becoming limiting, to avoid vibration issues due to the lowering of the blade passing frequency (Ref. **?**).

Propeller Design To attempt to optimise the design of the propeller, for some given flight condition, a simple design algorithm was developed. This design algorithm is largely based on the work of Adkins and Liebeck (Ref. **?**). The aim of the algorithm is to output a propeller design with the greatest achievable propulsive efficiency at some flight condition. Like the algorithm of Adkins and Liebeck (Ref. **?**), the user is required to input the radius of the propeller, its rotational speed and the amount of thrust the propeller is required to generate. Also, the user is required

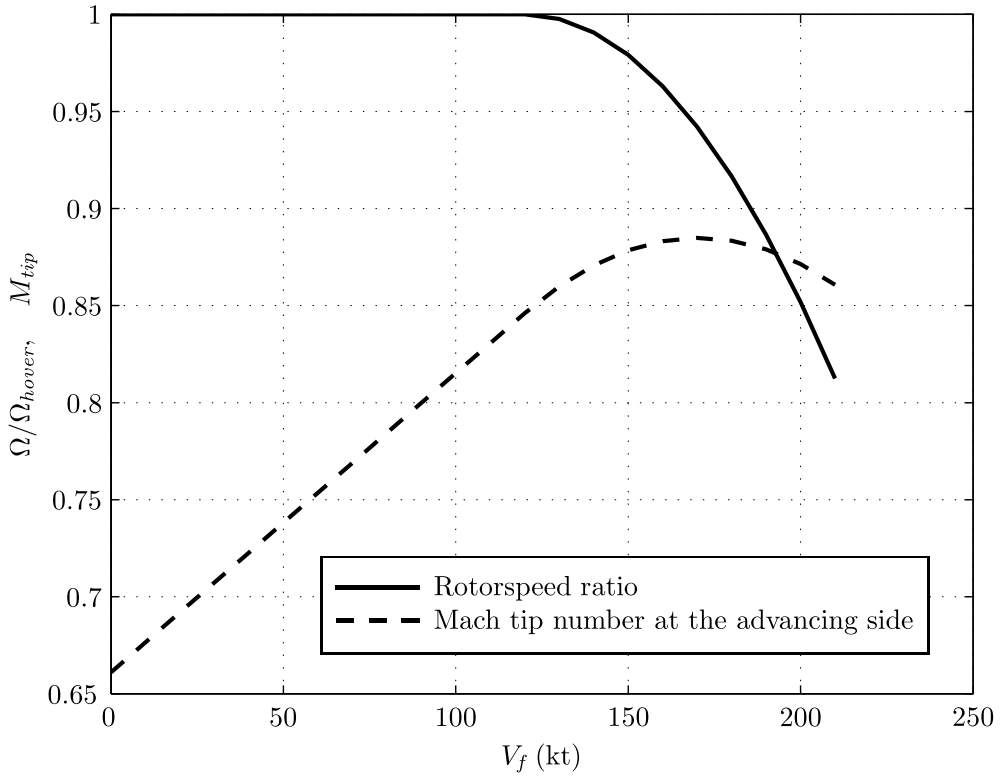

Fig. 3. Variation of Rotorspeed for the compound helicopter

to input the appropriate flight conditions such as airspeed, altitude density and glideslope. Essentially, the algorithm calculates two design parameters which are of critical importance to the propeller. The first parameter is the mean chord (or solidity) of the propeller to produce the required thrust. It is well understood that the profile power of the propeller is kept to a minimum when each blade section operates at an angle of attack where the local lift-to-drag ratio is maximised (Refs. **?**, **?**). Therefore, the second parameter calculated is the propeller twist to minimise profile power. The functions that the algorithm solves are:

$$T_{req} - T_{prod} = 0 \tag{2a}$$
$$\varepsilon_1 - \alpha_1 = 0 \tag{2b}$$
$$\varepsilon_2 - \alpha_2 = 0 \tag{2c}$$
$$\vdots$$
$$\varepsilon_n - \alpha_n = 0 \tag{2d}$$

where T_{req} is the required propulsive thrust and T_{prod} is the thrust produced by the blade element propeller model. The term ε is the local angle of attack where the maximum lift-to-drag ratio is achieved. The local angle of attack at each propeller blade station is given by α. The subscripts in the ε and α terms represents the radial station of interest. For example, α_1 is the angle of attack at the propeller station nearest the propeller hub. Note that n corresponds to the number of blade elements considered. Hence, α_n is the angle of attack at the section nearest the propeller tip.

Cheyenne Compound Propeller At the cruise condition the propeller of the Cheyenne Compound is required provide all of the propulsive thrust, as the main rotor is significantly offloaded. For a conventional helicopter the drag of the airframe may be approximated with

$$D_{af} = D_{fus} + D_{rot} + D_{tr} + D_{fin} + D_{tp} \tag{3}$$

Calculating the drag of each component can be a difficult challenge, therefore numerical predictions of helicopter drag are usually carried out using the equivalent flat plate area. Using this method the drag of the airframe, D_{af}, can be stated as

$$D_{flat} = \frac{1}{2}\rho V_f^2 f_e \tag{4}$$

where f_e is the equivalent flat plate area of the helicopter. Equation (**??**) can be used to predict the drag of the compound helicopter, however the addition of other aircraft components needs to be taken into account. Hence, the drag of the Cheyenne compound can be expressed as

$$D_{tot} = D_{flat} + D_{w,\,prof} + D_{w,\,ind} \tag{5}$$

where $D_{w,\,prof}$ and $D_{w,\,ind}$ represent the profile and induced drag of the wing, respectively. The assumption made here is that the compound helicopter will feature a modern airframe design which reduces the amount of drag. Ormiston suggests (Ref. **?**) that the equivalent flat plate area of modern designs can be approximated with

$$D_{flat} = 0.087\left(\frac{W}{1000}\right)^{2/3} \tag{6}$$

Using the aircraft mass of 7200 kg, then the flat plate area of the conventional helicopter is 1.49 m^2. The profile drag of the wing can be determined using a standard drag estimation technique, which is described in various design textbooks (Refs. **?**, **?**). The profile drag of the wing is given by

$$D_{w,\,prof} = \frac{1}{2}\rho V_f^2 S C_{D0} \tag{7}$$

where the amount of drag is captured by the zero lift drag coefficient, C_{D0}. Using the standard drag estimation method, the drag coefficient is approximated to be 0.01. The induced drag of the wing, $D_{w,\,ind}$, can be estimated using

$$D_{w,\,ind} = \frac{1}{2}\rho V_f^2 S C_{Di} \tag{8}$$

where C_{Di} is the induced drag coefficient which can be approximated using

$$C_{Di} = \frac{1}{AR\pi e} C_L^2 \tag{9}$$

The term e is the "Oswald efficiency factor", which is assumed to be 0.75. Using the cruise flight conditions then the total estimated airframe drag of the Cheyenne compound is 12600 N. Hence, at the cruise condition the pusher propeller is required to provide 12600 N of propulsive thrust. Typically, the highest achievable propulsive efficiency is about 0.86. Consequently, the goal here is to design a propeller with a propulsive efficiency, $\eta = TV/P$, of 0.86 at the cruise condition. Therefore, for the Cheyenne compound design the desired propeller power at cruise is 1582 kW.

Before applying the propeller design algorithm, the propeller's radius and rotational speed need to be determined. The propeller radius is determined by using historical data of modern propellers (Ref. **?**). Marinus and Poppe present

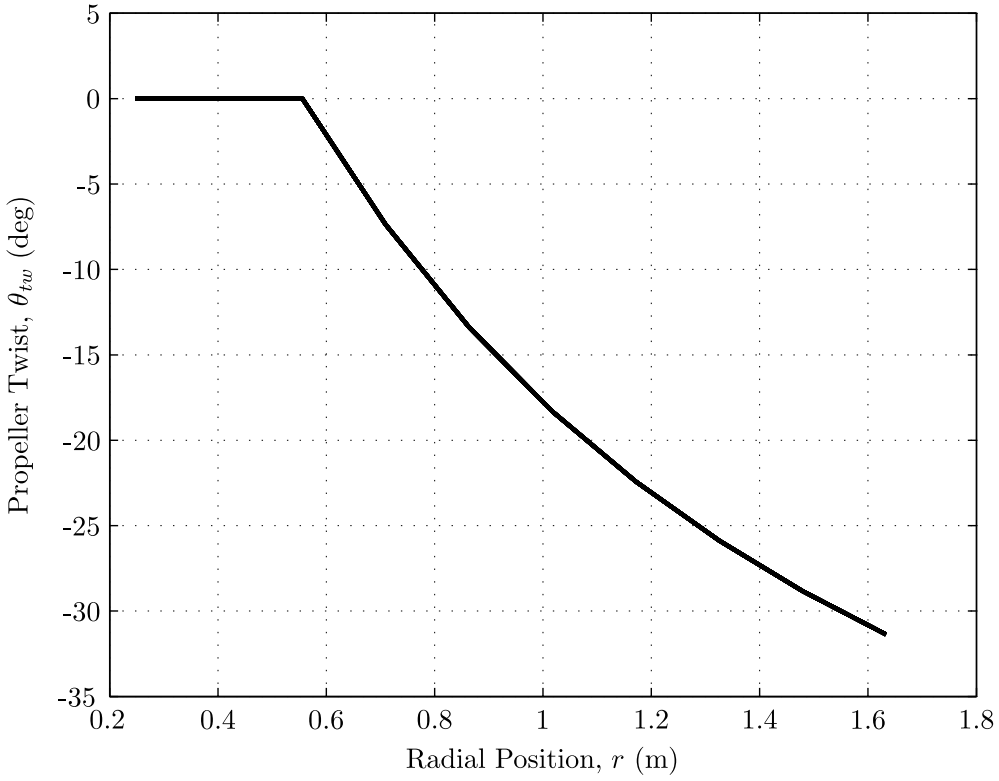

Fig. 4. Calculated Propeller Twist Distribution for the Cheyenne Compound

the historical relationship between the diameters of different propellers and the maximum shaft power (Ref. **?**). The maximum shaft power for the Cheyenne configuration is assumed to be 20% greater than the power required at cruise, to accommodate for emergency situations and aggressive manoeuvring flight. This gives a maximum shaft power of 1898 kW, therefore the propeller radius is predicted to be 1.71 m. The Mach tip number of the propeller should not exceed 0.87 at cruise, therefore the propeller's rotational speed is chosen to be 150 rad/s. Another design consideration is the choice of aerofoil sections. For this propeller design, the aerofoil selected is the NACA0012 aerofoil. The motivation for this aerofoil choice is that comprehensive "look-up tables" are available which allow the lift and drag coefficients to be calculated based on the local angle of attack and Mach numbers.

Some of the basic design parameters of the Cheyenne compound configuration have now been determined. Figure **??** shows the calculated optimum propeller twist distribution from the propeller design code. As expected, the propeller requires a large amount of negative twist to ensure a high propulsive efficiency at the cruise condition. The tangential velocity of each radial station changes significantly across the propeller blade, which requires a large amount of twist to optimise the angle of attack at each section. The tip of the propeller blade is pitched down by an angle of 31 deg, Figure **??**. The variation of twist is nonlinear, although it could be approximated to be linear if desired. Note it is assumed that the inner portion of the propeller blade, between the root and 32% across the blade, has zero twist. The thrust capability of this part of the blade is limited, therefore no attempt was made to optimise the twist at this portion of the blade.

Figure **??** shows the resultant angle of attack variation across the propeller blade at the cruise condition. The blade angle of attack, α_{bl}, changes in a linear manner towards the tip, Figure **??**. Note that towards the root there is a stall region due to the low local dynamic pressure, therefore these angles of attack are not shown in Figure **??**. The maximum lift-to-drag ratio of each radial station is dependent on the local Mach number, due to the effects of compressibility. It is well known that the drag coefficient of a typical aerofoil increases dramatically as the local Mach number approaches unity (Ref. **?**). As a result, the lower the Mach number, the higher the angle of attack where the maximum lift-to-drag ratio is achieved. This is shown in Figure **??**, with the highest angle of attacks occurring at the inner sections of the propeller blade. The angle of attacks begin to lower towards the outer portion

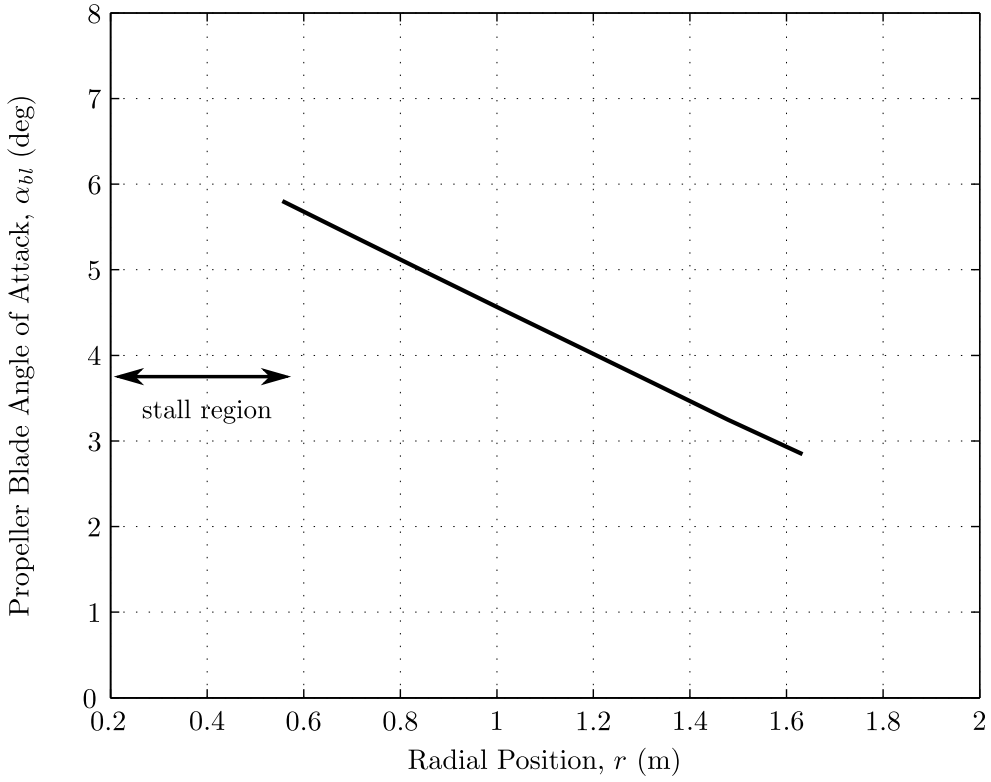

Fig. 5. Calculated Propeller Twist Distribution for the Cheyenne Compound

of the blade due to the effects of compressibility.

The result is a propeller planform with a high level of twist, which promotes favourable angles of attack across the blade at the cruise condition. The mean chord calculated by the propeller design algorithm is 0.258 m, giving a propeller solidity of 0.19. The propulsive efficiency at cruise is 0.85, which is close to maximum achievable efficiency. It is interesting to note than when compressibility effects are not modelled, by assuming linear aerodynamics, then the maximum propulsive efficiency achievable is 0.95. This is clearly unreasonable and reinforces the need to model compressibility effects to capture the performance of the propeller.

INVERSE SIMULATION ALGORITHM

The inverse simulation algorithm used is the so called integration method. This method is well documented in the literature (Refs. **?**, **?**, **?**), therefore only a brief description is provided in the main text. The integration method uses numerical integration and conventional simulation to calculate the controls required to move a vehicle through a desired trajectory (Ref. **?**). Essentially, inverse simulation reverses the process of traditional simulation, Figure **??**. The first step is to calculate the control angles that trim the aircraft for the given starting airspeed. Generally, a helicopter can be in trimmed flight when climbing, descending or flying with a lateral velocity (sideslip). However in this current work the trimmed state corresponds to steady level flight with the body accelerations and the attitude rates equal to zero. Concerning the UH-60A helicopter, the trim algorithm calculates the four control angles, roll and pitch angles which result in zero translational and angular accelerations acting at the aircraft's center of gravity. Essentially, there are six trim targets which are

Mission Task Element (MTE)

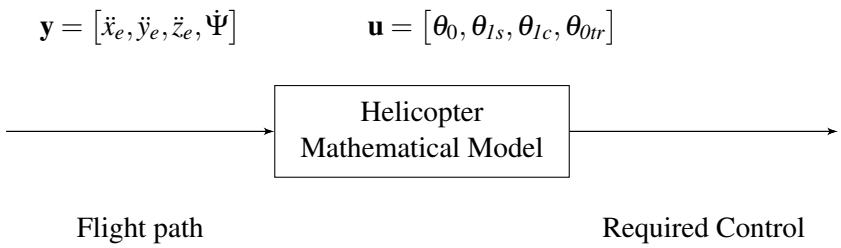

Fig. 6. Schematic showing the process of Inverse Simulation

$$X - mg\sin\Theta \tag{10}$$
$$Y + mg\cos\Theta\sin\Phi \tag{11}$$
$$Z + mg\cos\Theta\cos\Phi \tag{12}$$
$$L = 0 \tag{13}$$
$$M = 0 \tag{14}$$
$$N = 0 \tag{15}$$

which correspond to the condition of steady level flight. However, the introduction of an extra control to the Cheyenne compound requires a slightly different approach to trim these vehicles. The Cheyenne configuration features five controls and a description of the controls is shown in Table **??**. There are two approaches taken to determine the control angles required to trim the compound helicopter. The first method trims the compound helicopter in low speed flight, whereas the second calculates the trim controls in forward flight. In low speed flight, an additional trim constraint is added, to make a total of seven trim targets. This additional constraint is to match the propulsive thrust of the propeller(s), depending on the compound configuration, to a prescribed thrust value. This approach minimises the power of the propeller(s) in low speed flight. For the Cheyenne configuration, the additional constraint is

$$T_{prop} = X \tag{16}$$

This constraint (or trim target) is added to the six trim targets, Equations (**??**) - (**??**), making a total of seven trim targets to match the seven unknowns. The term X in Equation (**??**) is a prescribed thrust value which is selected to minimise the power of the propellers in low speed flight.

In forward flight the trim algorithm is switched to a different approach. The pitch attitude of the compound helicopter is fixed to a zero pitch attitude, $\Theta = 0$ deg, in forward flight. The choice to constraint the compound helicopters to a level fuselage is an attempt to minimise the drag of the fuselage and to ensure that the aircraft's wing operates close to its maximum lift-to-drag ratio. The angle of incidence of the wing is selected to be 7 deg, for the compound vehicle, which gives a lift coefficient of the wing, C_L, of approximately 0.6 in forward flight. This results in the wing of the compound providing a significant amount of lifting force whilst retaining an adequate stall margin, at low drag. An indirect consequence of this trim approach is that the two propellers provide the majority of propulsive force to overcome the airframe drag in high speed flight.

The next step, after the calculation of the trim control angles, is to define the manoeuvre. The manoeuvre is discretised into a series of discrete time points, t_k, by specifying the time step. Subsequently, the manoeuvre can be determined with a matrix, $\boldsymbol{y}_{des}(t_k)$ representing the flight path of the manoeuvre. The manoeuvre can be defined

Control Symbol	Control Name	Control Axis
θ_0	Main rotor collective	Heave control
θ_{1s}	Main rotor longitudinal cyclic	Pitch control
θ_{1c}	Main rotor lateral cyclic	Roll control
θ_{prop}	Propeller pitch	Propeller thrust control
θ_{tr}	Tail-rotor pitch	Yaw control

Table 2. Controls for the Cheyenne Compound Configuration

by polynomials that satisfy the requirements of the particular manoeuvre (Ref. **?**), with the mathematical modelling of the Depart and Abort manoeuvre detailed later. Starting from the trimmed condition, $\boldsymbol{u}_e$ is the initial guess to calculate the control vector, $\boldsymbol{u}$, to force the helicopter to the position of the next time point. A Newton-Raphson technique is used to calculate the control vector to force the vehicle to the next time point to match the desired flight path defined by $\boldsymbol{y}_{des}(t_k)$. After convergence, this numerical technique moves onto the next time point and repeats the process. The end result is the control activity required throughout the manoeuvre.

MANOEUVRE MODELLING

To successfully implement inverse simulation, the trajectory the aircraft is to follow is required. In the early inverse simulation algorithms, the output vector $\boldsymbol{y}_{des}$, which describes the trajectory, was defined as follows:

$$\boldsymbol{y}_{des} = \begin{bmatrix} x_e & y_e & z_e & \Psi \text{ or } \beta \end{bmatrix}^{\mathrm{T}} \tag{17}$$

where x_e, y_e and z_e are the flight path co-ordinates and the additional constraint is either the heading or sideslip angle. As previously stated, the integration method is a flexible and robust approach to solve the inverse problem. However, the development of this approach provided new numerical instabilities, such as the control activity featuring "low-amplitude, high frequency oscillations superimposed on the low frequency waveform" as discussed by Hess, Gao and Wang (Ref. **?**). Originally, the desired output vector was composed of the flight path co-ordinates with an additional constraint, either the heading or sideslip angles, as seen in Equation (**??**). However, Rutherford and Thomson showed that altering the output vector to be compose of inertial accelerations removed the high frequency oscillations of the control activity (Ref. **?**). Therefore, modifying the output vector to the following

$$\boldsymbol{y}_{\text{des}} = \begin{bmatrix} \ddot{x}_e & \ddot{y}_e & \ddot{z}_e & \dot{\Psi} \text{ or } \dot{\beta} \end{bmatrix}^{\mathrm{T}} \tag{18}$$

was shown to attenuate these oscillations (Ref. **?**). Consequently, in this current work the output vector consists of the aircraft accelerations and heading or sideslip rate. The accelerations are determined by the differentiation of the velocities in Earth axes. The velocities, in Earth Axes, are conveniently described by the trajectory angles (glideslope and track angles) as seen in Figure **??**. The velocities, are therefore given by

$$\dot{x}_e = V\cos\gamma\cos\chi \tag{19}$$
$$\dot{y}_e = V\cos\gamma\sin\chi \tag{20}$$
$$\dot{z}_e = -V\sin\gamma \tag{21}$$

leading to the following accelerations

$$\ddot{x}_e = \dot{V}\cos\gamma\cos\chi - V\dot{\gamma}\sin\gamma\cos\chi - V\dot{\chi}\cos\gamma\sin\chi \tag{22}$$
$$\ddot{y}_e = \dot{V}\cos\gamma\sin\chi - V\dot{\gamma}\sin\gamma\sin\chi + V\dot{\chi}\cos\gamma\cos\chi \tag{23}$$
$$\ddot{z}_e = -\dot{V}\sin\gamma - V\dot{\gamma}\cos\gamma \tag{24}$$

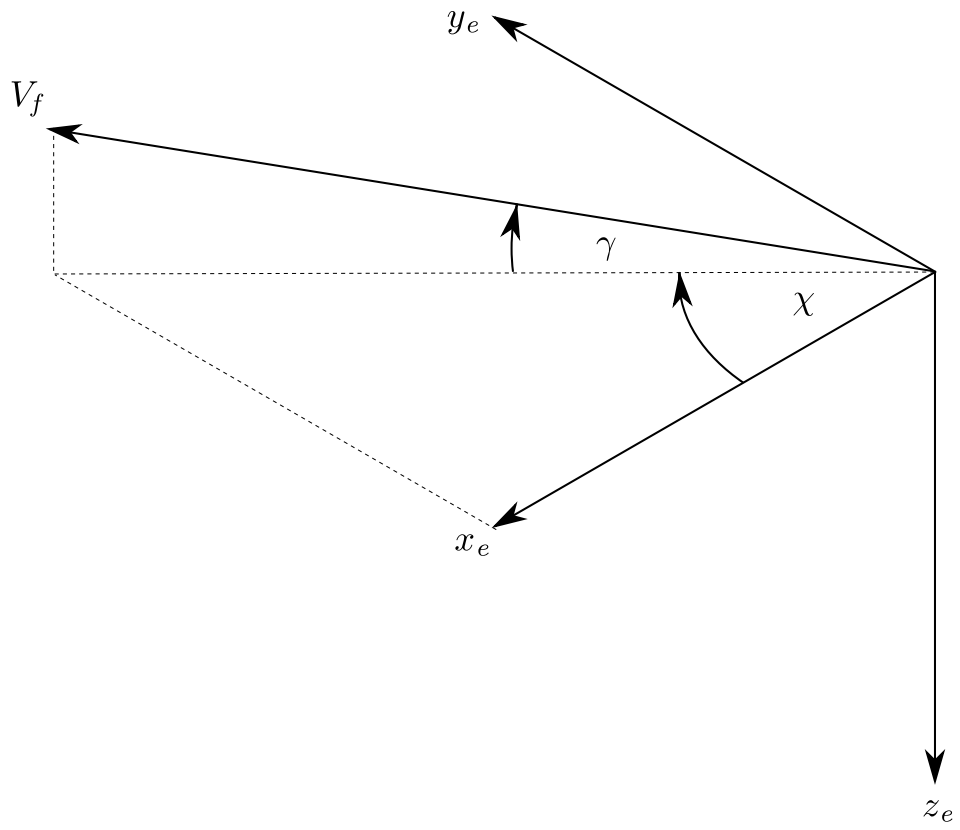

Fig. 7. Diagram showing the definition of the glideslope and track angles

Therefore if γ, χ and V are all defined and their time derivatives calculated, then the accelerations can be determined, hence forming the output vector.

Alternatively, the accelerations in Earth axes may be known from flight test data. This is for the case for the Depart and Abort manoeuvre. The flightpath was obtained from flight tests conducted the US Army's research centre at Moffet Field (Ref. **?**). The helicopter's position throughout the manoeuvre were taken and discretised using the appropriate time step. Thereafter, the aircraft's position was differentiated twice to obtain the helicopter's accelerations in the Earth axes set.

Justification of the Manoeuvre Selection

In theory, inverse simulation can be used to calculate the control activity required to fly any manoeuvre, with the assumption that an appropriate output vector, Equation (**??**), can be formed. There are a wide selection of manoeuvres which helicopters are required to perform routinely. In this study, the manoeuvre selection is based on two factors. Firstly, it seems prudent to select a manoeuvre where the addition of compounding is likely to have a significant influence. The second factor in the selection of the manoeuvre is the fidelity of the helicopter mathematical model. As discussed in the Section **??**, the level 1 simulation model (which is the focus of the study) is not suitable for flight regimes where the main rotor aerodynamics become highly nonlinear due to compressibility and reverse flow effects. Hence, the selected manoeuvre should begin and end when the helicopter is operating well within its Operational Flight Envelope (OFE). As a consequence, the use of a level 1 model prohibits the use of the inverse simulation algorithm in high speed flight. The use of the Level 2 simulation model would be required to assess the compound helicopters at the edge of their perceived flight envelope.

To satisfy the these conditions, the study focuses on the Depart and Abort test manoeuvre, which is described in the ADS-33 specification (Ref. **?**). An additional benefit of the Depart and Abort manoeuvre is that the research team have access to flight test corresponding to this particular manoeuvre. The main aim of the Depart and Abort

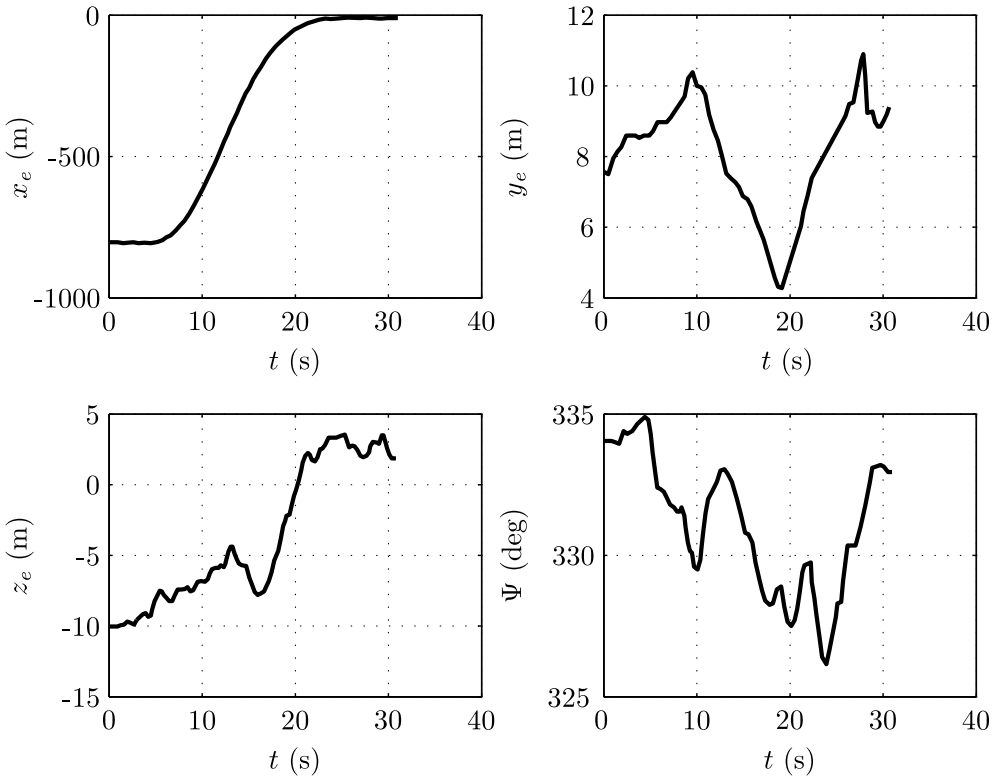

Fig. 8. Flight path of the Depart and Abort Mission

manoeuvre is to test the aircraft's pitch and heave axis handling qualities (Ref. **?**). One undesirable effect of the conventional helicopter, is the large pitch excursions required to accelerate the aircraft. As the main rotor is the sole source of propulsion for a conventional helicopter, the rotor is required to tilt forward so that a component of the rotor thrust vector provides a propulsive force. This tilt of the main rotor also comes with the penalty of pitching the aircraft's nose down. However, the introduction of thrust compounding offers the potential of reducing the pitch excursion, as the propeller can provide the required propulsive force. There are also questions relating to the design of the propeller. For example, how much propulsive force can thrust compounding provide during the Depart and Abort test manoeuvre? Also, what is the best control strategy to fly this manoeuvre? Overall, there are a variety of research questions, which this study attempts to answer.

Although only the Depart and Abort manoeuvre is considered in this study, it is possible that this work could be extended to investigate the performance and handling qualities of compound helicopters in high speed manoeuvres. The natural consequence of compounding the helicopter is the expansion of the flight envelope, exposing the helicopter to unfamiliar flight conditions. Consequently, the compound helicopter will be able to perform high speed level turns or high-speed pull ups. These types of manoeuvres should be considered in future studies. An investigation of these types of manoeuvres would need to be supported by a level 2 rotor model, which is capable of modelling nonlinear aerodynamics such as retreating blade stall and compressibility effects. Lateral-directional manoeuvres, such as the slalom, could also be considered in future studies. The addition of propeller(s) to the helicopter's airframe will generate gyroscopic moments when the helicopter is pitching, rolling or turning. These moments could degrade the handling qualities of the vehicle and this type of study could provide some interesting results. Another issue is that compound helicopters typically do not have a conventional tail-rotor, meaning that the yaw control of the vehicle is provided by some other mechanism. Therefore, a manoeuvre like the slalom could potentially be used to compare the effectiveness of the devices which are used for yaw control.

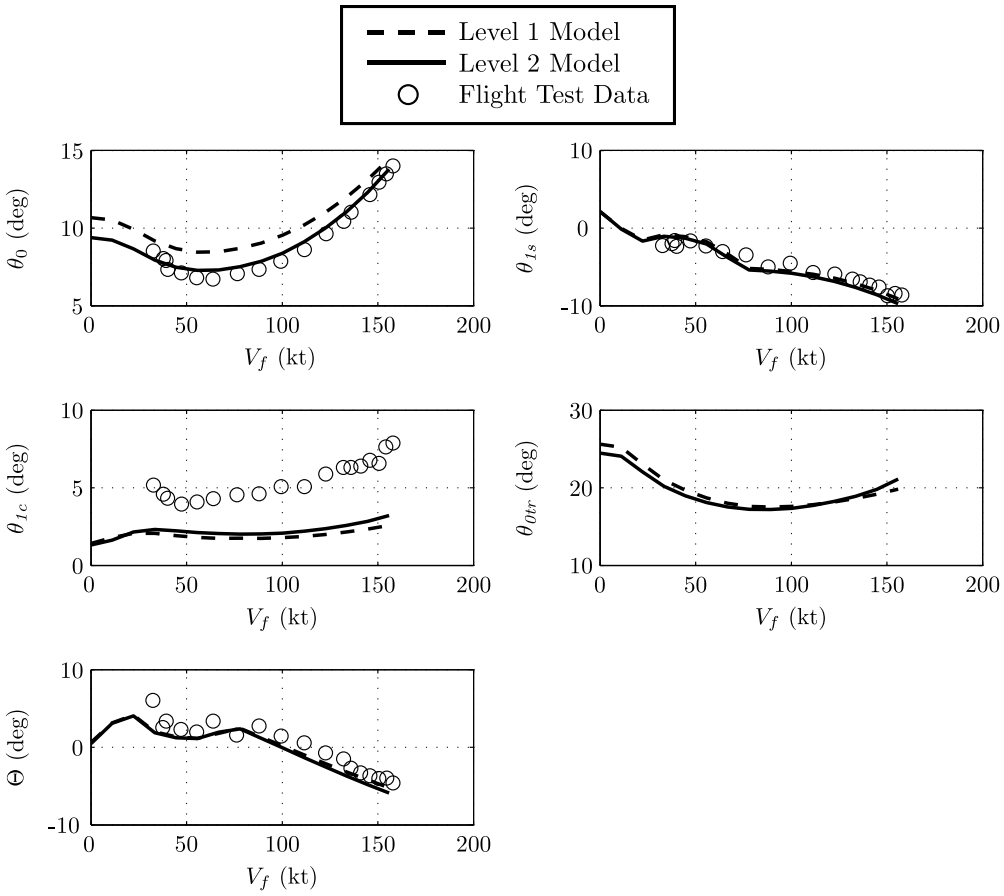

Fig. 9. UH-60A Trim Results using the Levels 1 and 2 Mathematical Models

RESULTS

Validation of the UH-60A Model

One of the first tasks is to compare the conventional helicopter simulation model with flight test data, in order to gain confidence of the mathematical model. Fortunately, there is data available from UH-60A flight tests which can be used for model validation (Refs. **?**,**?**). The UH-60A simulation model is trimmed and compared with results from the flight test designated FLT-85 (Ref. **?**). The results are shown in Figure **??**, and the agreement between the simulation and flight test data is generally very good. Also shown is the comparison between the two simulation models, the levels 1 and 2 models, which were introduced in Section **??**. The level 1 model over-predicts the collective angle across the flight envelope. For the level 2 model (the model which includes nonlinear aerodynamics), the comparison between the collective angle and the corresponding flight test results is excellent. It is important to note that the results above 130 kt, where blade stalling may occur, is excellent. The level 2 does not include a dynamic stall model, but it doesn't seem to adversely influence the trim results. Despite this, it is recognised that dynamic stall is important aerodynamic phenomenon, particularly in aggressive manoeuvring flight, and it is recommended a dynamic stall model is included into the simulation model, at a later date. The prediction of the longitudinal cyclic angles, using both the levels 1 and 2 models, is excellent across the entire flight envelope. This result is particularly impressive considering the moveable tailplane of the UH-60A, with the UH-60A simulation model successfully modelling its effect to the pitch axis. The variation of the tailplane's incidence is why the longitudinal cyclic changes quite abruptly at some parts of the flight envelope. As expected, the pitch attitude results are also excellent. There is quite a large difference between the lateral cyclic results, Figure **??**. This also occurs in another modelling study (Ref. **?**), which uses the state of the art model, CAMRAD II. The reason for the disparity of the lateral cyclic results is unknown. Unfortunately, the data recorded in FLT-85 does not include the tail-rotor collective

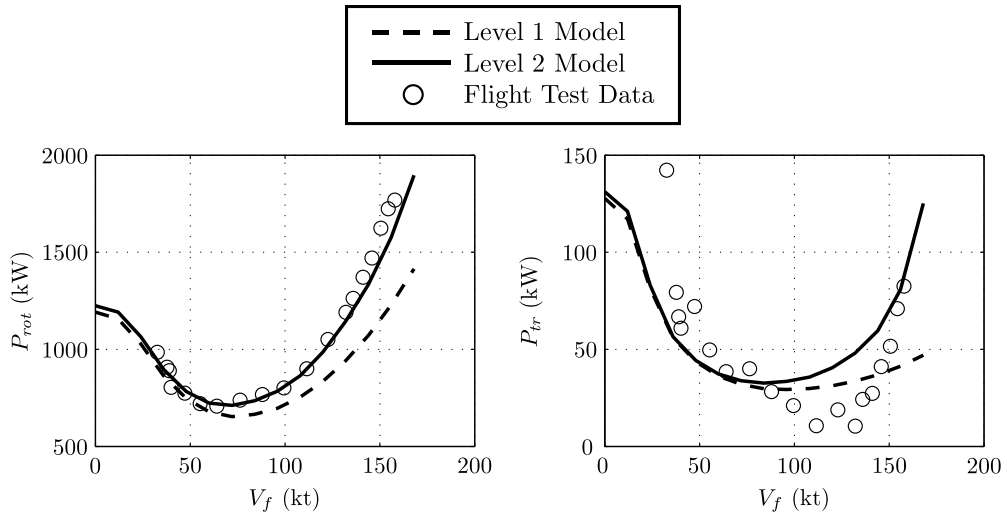

Fig. 10. UH-60A Power Predication using the Levels 1 and 2 Mathematical Models

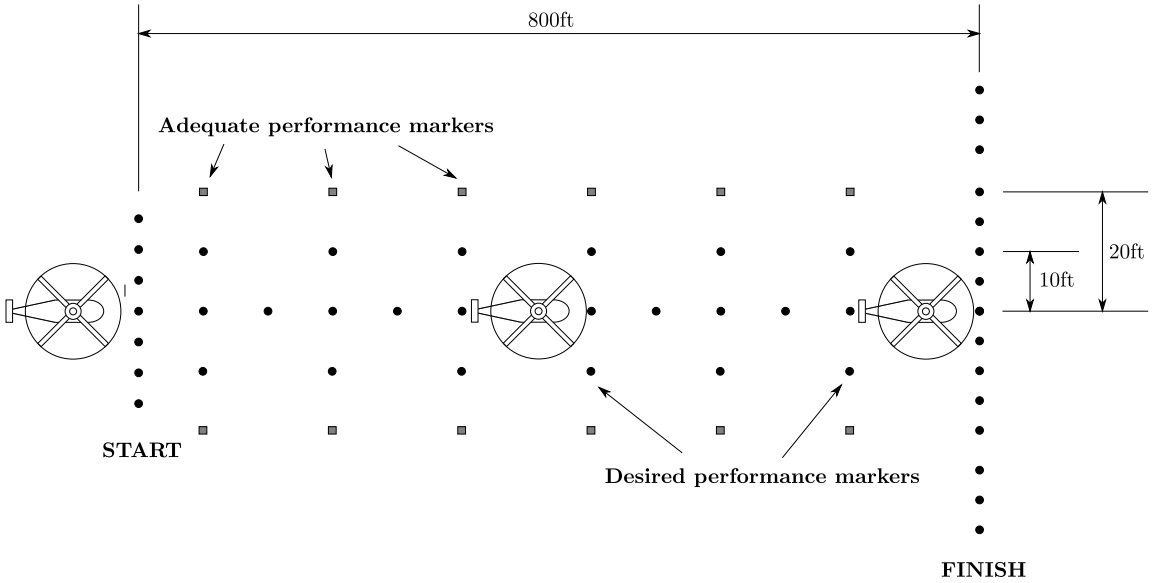

Fig. 11. Depart and Abort Test Course from ADS-33 (Ref. ?)

results.

Figure **??** compares the main rotor and tail-rotor power results with the flight test data from FLT-85. For the main rotor's power, the results of the level 2 model show excellent agreement across the whole flight envelope. In terms of the level 1 model, the results compare favourably with the flight test data, but only between the hover and 70 kt. Thereafter, the level 1 model under-predicts the main rotor power. The level 1 model assumes that the profile drag per blade element is based on a constant drag profile coefficient. As a result, this model is incapable of successfully predicting the main rotor's profile drag rise in forward flight, due to its inability to model nonlinear aerodynamics. In contrast, the level 2 model is capable of modelling compressibility effects and blade stalling, by using comprehensive look-up tables of the SC-1095 aerofoil (Refs. **?**, **?**). The end result here is that a level 2 model is required to successfully predict the main rotor's power in forward flight. In terms of the tail-rotor power, both models compare favourably with the flight test data until an airspeed of 70 kt. After 70 kt, both models do not predict the tail-rotor power well. These differences are also observed in the work of Yeo and Johnson (Ref. **?**), and the reason for the disparity is unclear.

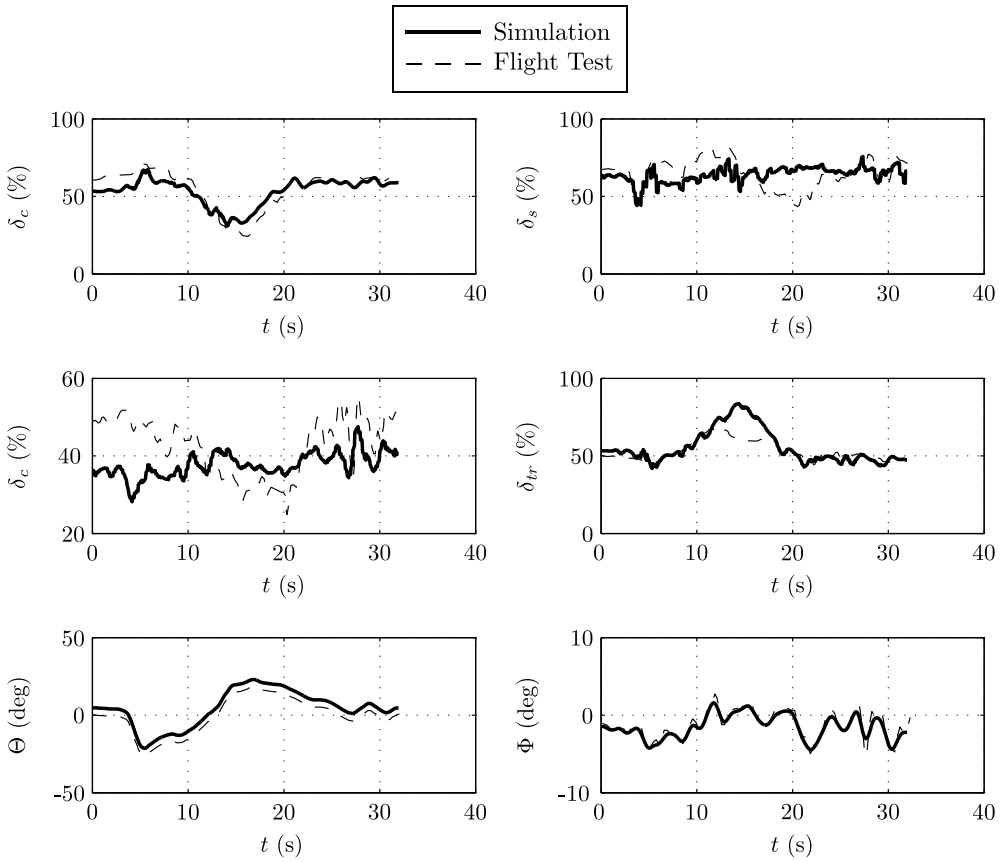

Fig. 12. Comparison between the Control Positions during the Depart and Abort Test Manoeuvre

The level 1 simulation model has been validated in steady level flight, and some issues with the model have been identified. A more rigorous test of the simulation model is to calculate the control angles in manoeuvring flight and compare them with flight test data. Fortunately, one of the benefits of inverse simulation is that it is possible to fly the simulation model through a manoeuvre which is identical to a flight test trial, and then compare time histories (Ref. **?**). The manoeuvre of interest is the Depart and Abort MTE, and the corresponding test course is shown in Figure **??**. On the test course, Figure **??**, there are a series of cones placed to define the adequate and desired performance standards. In this task the helicopter starts in the hover and is required to accelerate forward to an airspeed of 40 kt, then return to a stabilised hover at the end of the 800 ft long course. The manoeuvre is only concluded when the pilot manages to place the helicopter's cockpit within 20 ft of the end point of the test course. Figure **??** shows the level 1 simulation model results of the UH-60A Blackhawk helicopter, flying the Depart and Abort MTE. The results from the simulation are compared with flight data from US Army flight trials (Ref. **?**). The US Army flight trial results where obtained in clear weather conditions during the summer of 1999 (Ref. **?**). The results are encouraging, particularly the agreement with the main rotor collective and the pedal inputs. The longitudinal and lateral stick movements are fairly well predicted, although there are some discrepancies between the simulation and flight test results. The agreement between the pitch and roll attitudes of the aircraft are excellent. Overall, the agreement is very good, highlighting that the level 1 simulation model, coupled with the inverse simulation algorithm, can be used to successfully predict the behaviour of the helicopter during this low speed test manoeuvre.

DEPART AND ABORT RESULTS

The process to calculate the conventional helicopter's controls through a manoeuvre was described earlier, and a schematic of the inverse simulation algorithm is reproduced in Figure **??**, to support the discussion. To apply

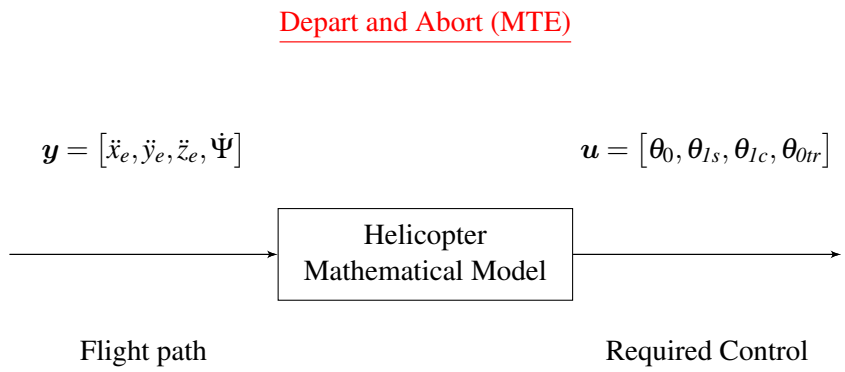

Fig. 13. Schematic showing the process to calculate the control of the Conventional Helicopter

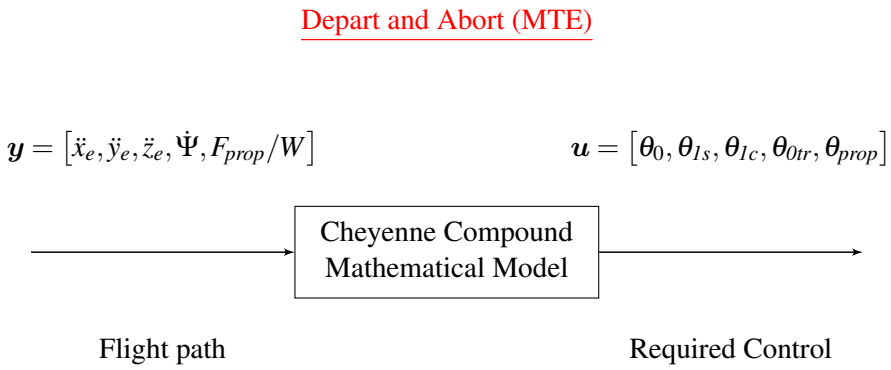

Fig. 14. Schematic showing the process to calculate the controls of the Cheyenne configuration

the inverse simulation algorithm successfully, the amount of unknowns must match the number of inputs. This occurs with the conventional helicopter, as there are four inputs, which define the manoeuvre, and four control angles to be calculated, Figure **??**. Since the compound helicopter feature five controls, an additional constraint is required, so that there are five inputs which match the five unknown controls. A logical question which arises with the compound helicopter flying the Depart and Abort manoeuvre is how much of the propulsive force is provided by the propellers. Conveniently, the fifth constraint for this manoeuvre is selected to be the ratio between the propeller's propulsive force (i.e. the force in the x_e direction) and the aircraft's weight. This allows the simulation to regulate how much propulsive force thrust compounding is required to create throughout the manoeuvre. For the Cheyenne compound, the inverse solution is shown in Figure **??**. There are five inputs into the inverse simulation algorithm: three accelerations, the heading angle and the ratio between the propulsive force the propeller is required to generate and the vehicle's weight. The algorithm subsequently calculates the five controls for this vehicle to fly this manoeuvre in the appropriate manner, Figure **??**.

It is likely that in the acceleration phase of the Depart and Abort manoeuvre that the pilot or control system would adopt a control strategy which would actively use thrust compounding to provide some portion of the propulsive force throughout the manoeuvre. However, it is unknown how much thrust the propellers are able to provide. Secondly, it is not known what is the optimum control strategy to minimise the power required by each compound configuration. As a result, the amount of propulsive thrust provided by the propellers is varied in multiple simulation runs to determine how sensitive the power required is to the control strategy adopted. The amount of thrust required by the propellers is gradually increased to the point where the propellers are incapable of producing the required thrust. Figure **??** shows how the ratio between the propulsive force, required by thrust compounding, and the aircraft's weight changes with each simulation run. The propulsive force ratio (F_{prop}/W) is formed by creating an 8th order polynomial as follows

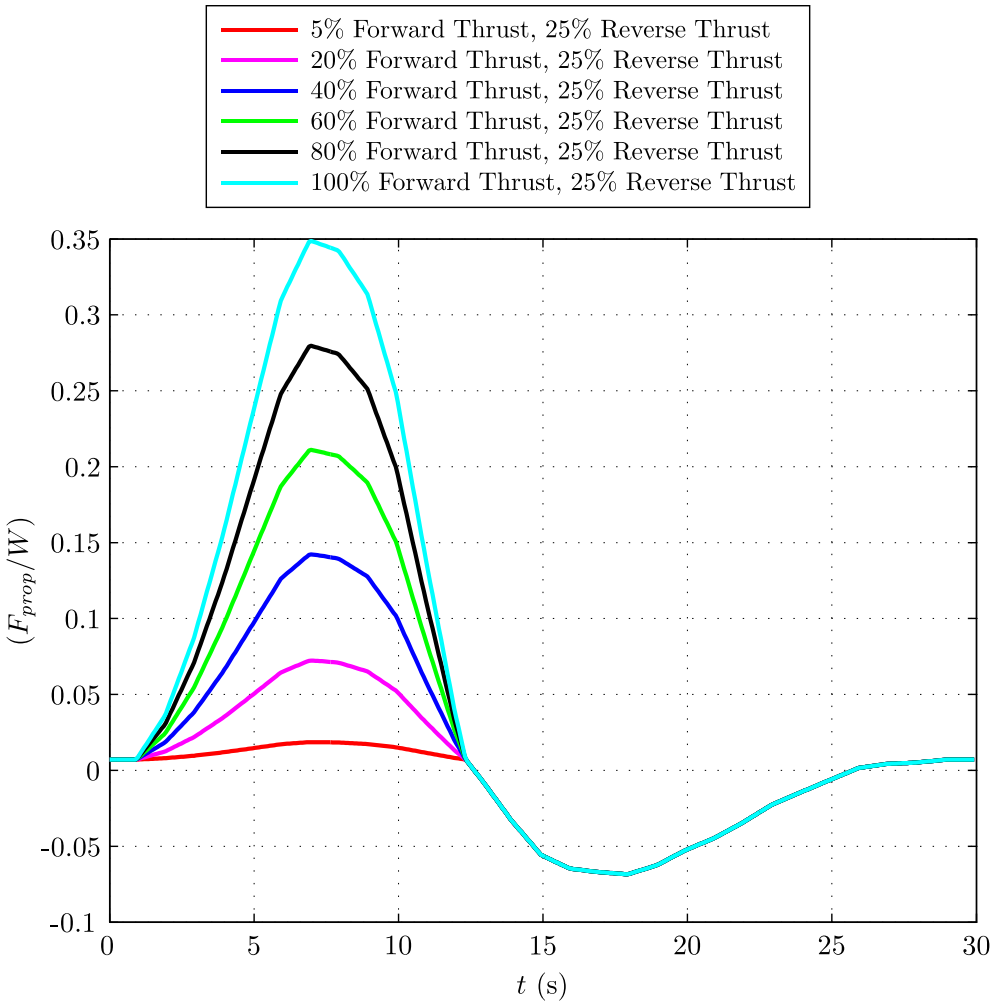

Fig. 15. Propulsive Force Provided by Thrust Compounding

$$\frac{F_{prop}}{W} = c_0 t^8 + c_1 t^7 \ldots c_7 t + c_8 \tag{25}$$

where c_0, c_1, etc. are coefficients. The coefficients of Equation (**??**) can be easily altered to promote greater propulsive thrust throughout the manoeuvre. Returning to Figure **??**, the first case (shown in red) is the minimal propulsive thrust case where the thrust compounding is not required to provide any meaningful propulsive thrust during the forward acceleration part of the manoeuvre. In this scenario, the compound helicopter flies the first part of the manoeuvre with traditional like helicopter manoeuvring. For the second case (which is shown in magenta) thrust compounding is required to provide more of the total propulsive thrust at the point of maximum forward acceleration, which occurs at 7 s. The amount of the propulsive thrust generated by thrust compounding is gradually increased until some aerodynamic restriction is met, Figure **??**. An additional advantage of thrust compounding is the possibility of using the propellers to decelerate the aircraft by providing reverse thrust. It is fair to assume that the design of the propellers would be optimised for high speed flight and not for reverse thrust purposes where the propellers operate in the windmill brake state. Hence it is assumed that the propellers provide 25% of the entire reverse force required to decelerate the vehicle at the time of peak deceleration. For every case, the amount of reverse thrust create by thrust compounding is 25%. Note that no comprehensive investigation was conducted to investigate the optimal amount of reverse thrust, and this is a recommendation for future work.

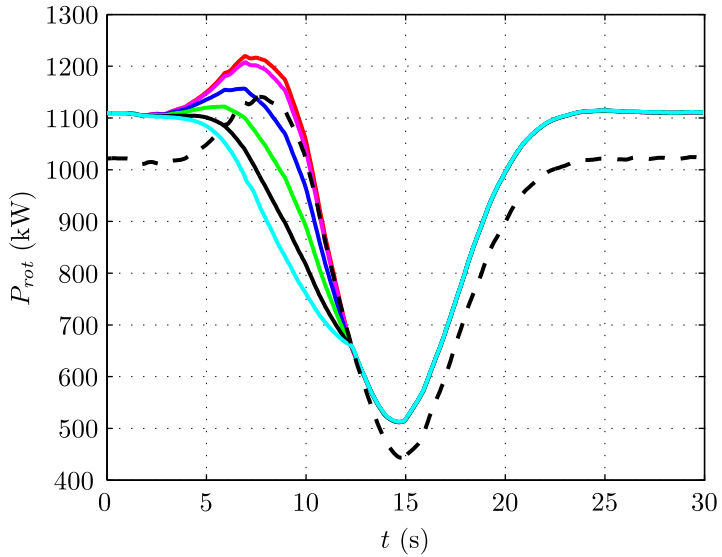

(a) Main Rotor Power

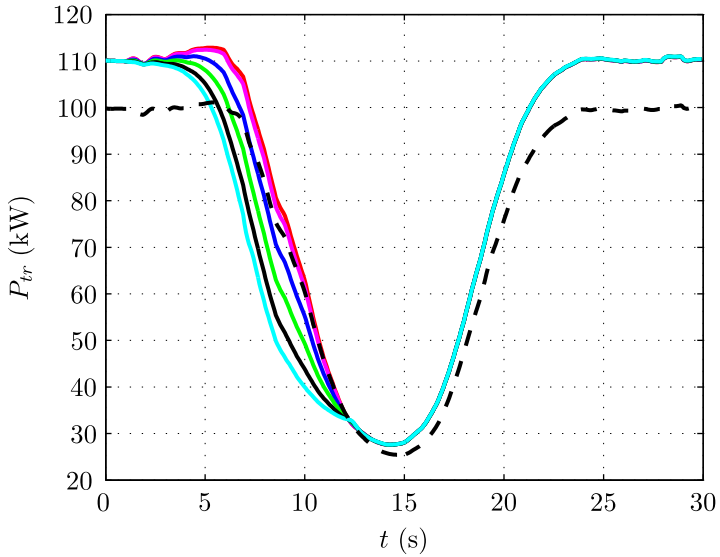

(b) Tail-rotor Power

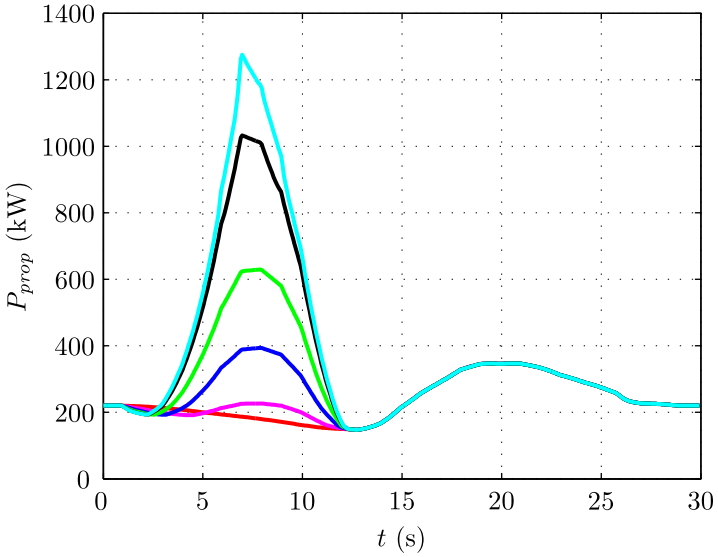

(c) Propeller Power

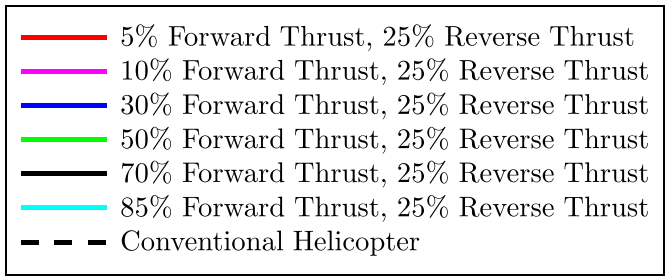

Fig. 16. Power Requirements of the Cheyenne Configuration

Cheyenne Configuration Results

Figure **??** (shown on the previous page) presents the power of the main rotor, tail-rotor and pusher propeller during the Depart and Abort manoeuvre for the various test cases considered. The results shown in Figure **??** correspond to the Cheyenne configuration with a pusher propeller of solidity 0.19. This solidity value was determined early in the study by focusing on the cruise condition of the Cheyenne configuration. It is predicted that the original propeller design of Cheyenne configuration is incapable of producing enough thrust to provide the entire propulsive force during the forward acceleration part of the manoeuvre. The result is that the propeller of the Cheyenne can only produce 85% of the total propulsive thrust to accelerate the aircraft forward, before the propeller suffers from blade stalling. Consequently, Figure **??** presents the test cases where the pusher propeller of the Cheyenne provides 5, 10, 30, 50, 70 and 85% of the propulsive thrust during the first part of the manoeuvre. The main rotor power is shown in Figure **??** and follows the expected trend. When comparing the 85% case of the Cheyenne compound, to the conventional helicopter, greater rotor power is required by the conventional helicopter between 6-12 s. This is due to the pusher propeller significantly offloading the main rotor of its propulsive duties. Although this is favourable, in terms of reducing the main rotor's power, there is a large increase to the power required by the pusher propeller, Figure **??**. In the deceleration part of the manoeuvre, between 12-30 s, there is a slight rise to the amount of power required by the pusher. This is due to the pusher propeller providing some of amount reverse thrust to slow the airspeed of the aircraft. For the Cheyenne compound, the power of the tail-rotor is fairly insensitive to the different test cases. As expected, as the pusher propeller is required to provide more thrust to accelerate the helicopter forward,

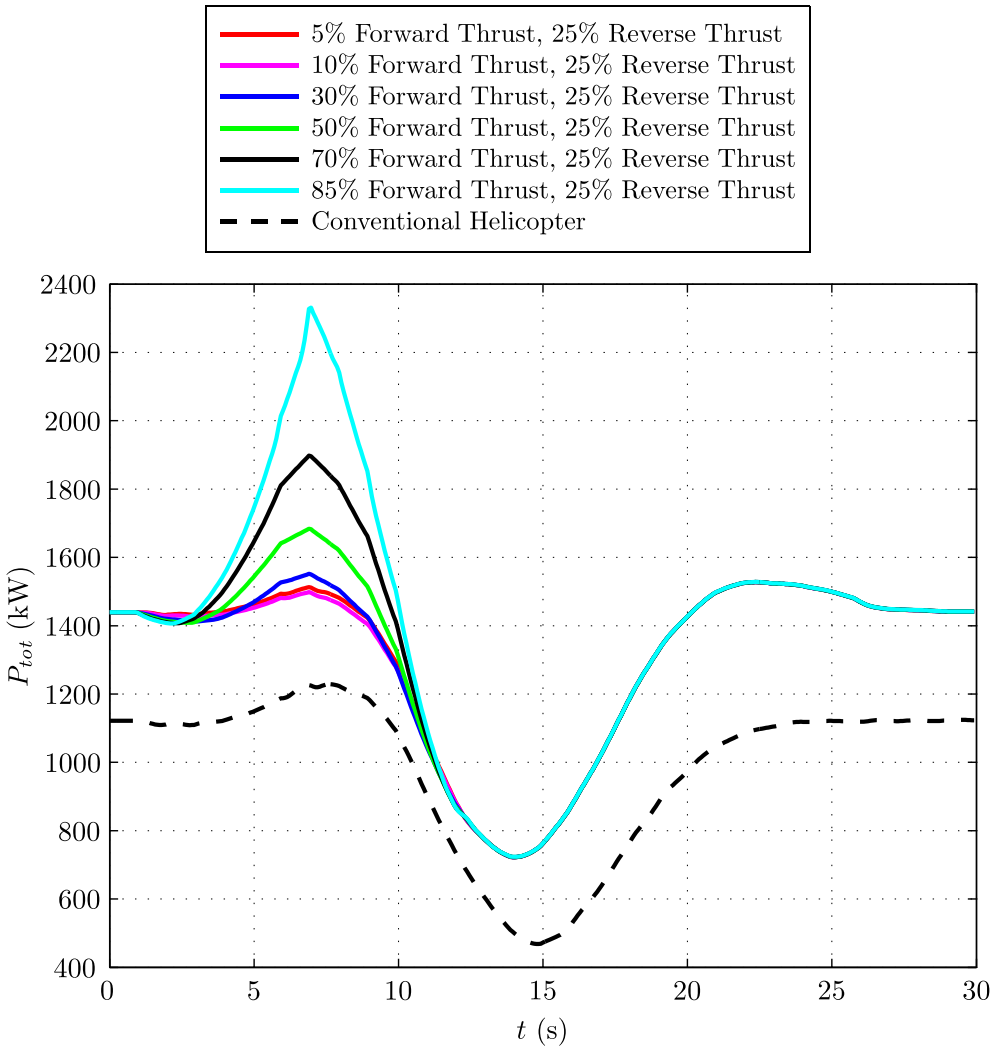

Fig. 17. Total Power Requirements of the Cheyenne Compound with a Propeller Solidity of 0.19

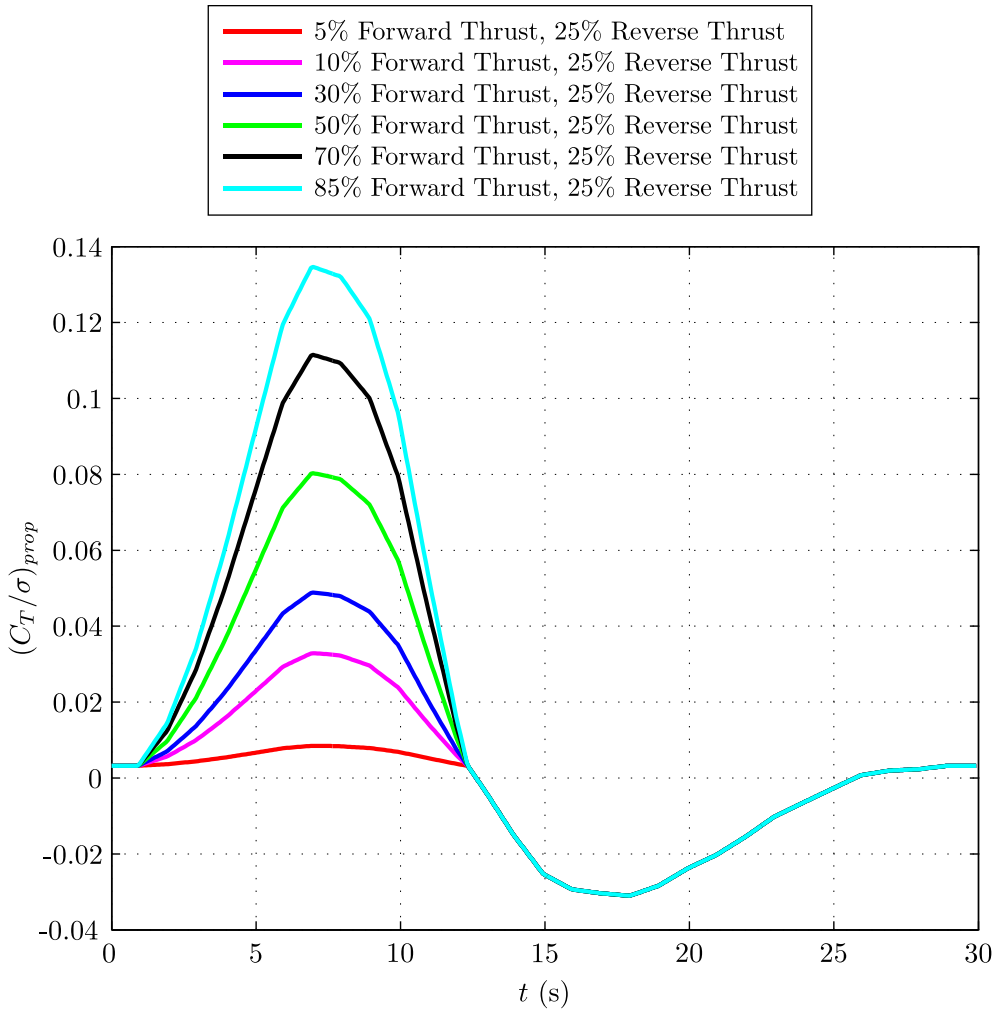

Fig. 18. Blade Loading of the Cheyenne Compound's Propeller using a Solidity of 0.19

the propeller power increases, Figure **??**.

Figure **??** presents the total power required by the Cheyenne compound with a propeller solidity of 0.19. For this particular configuration, the results show that the most efficient way to accelerate the aircraft forward, from the hover, is to minimise the amount of propeller thrust required by the pusher propeller. For the 5, 10 and 30% cases, there is little difference between the amount of power required to accelerate the Cheyenne forward. However, as the pusher propeller is required to contribute to more than 30% of the propulsive force, there is a general rise of the amount of power required between 3-11 s. This result further emphasises the ability of the conventional main rotor to efficiently produce a propulsive force in low speed flight. This is clearly demonstrated in Figure **??** by comparing the total power required by the conventional helicopter and the Cheyenne compound's 80% case, at 7 s. For the conventional helicopter, the total power required is 1207 kW, compared to the 2310 kW required by the Cheyenne configuration. This is a significant difference and suggests that if the Cheyenne compound were to fly the manoeuvre in this manner then it would require more installed power, than the conventional helicopter. Another general point worth highlighting is that the power required by the Cheyenne configuration is greater than that of the conventional throughout the entire manoeuvre, regardless of the test case considered.

As mentioned previously, with the current design, the pusher propeller is only capable of producing 85% of the total propulsive force during the forward acceleration part of the manoeuvre. Figure **??** presents the blade loading of the pusher propeller the Depart and Abort manoeuvre. The maximum blade loading value of the pusher propeller is achieved at the point of maximum forward acceleration, at approximately 7 s. As the aircraft begins to decelerate, the pusher propeller provides some reverse thrust which can be seen with the negative blade loading values after 12 s. The propeller of the Cheyenne compound's pusher propeller reaches its maximum thrust capability when

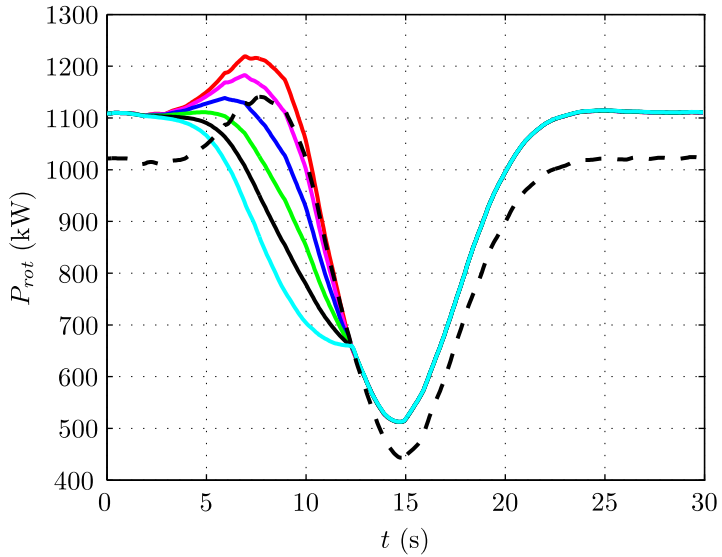

(a) Main Rotor Power

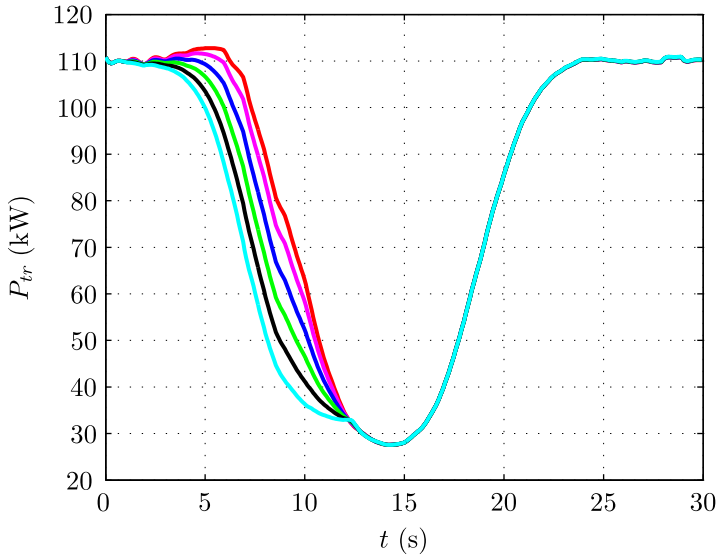

(b) Tail-rotor Power

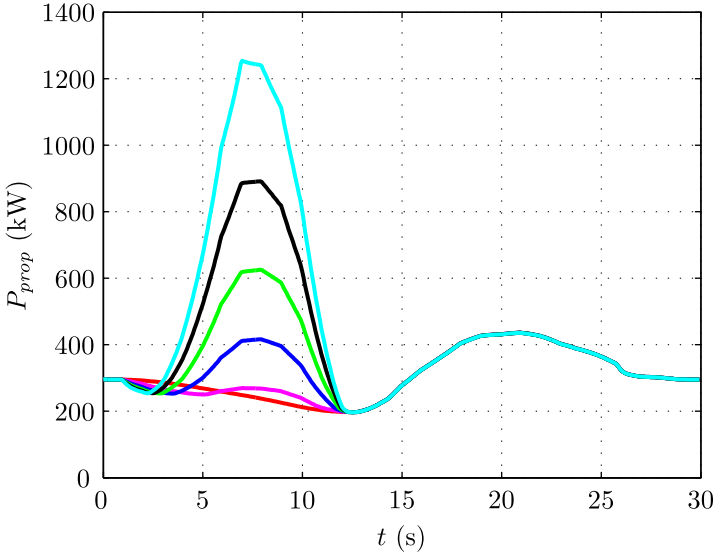

(c) Propeller Power

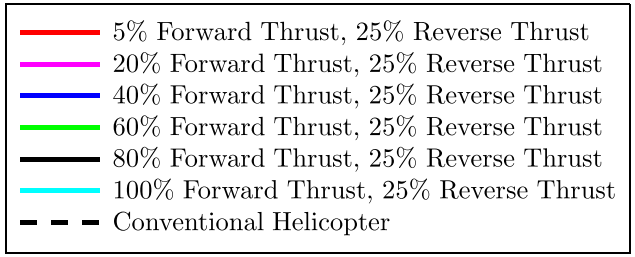

Fig. 19. Power Requirements of the Cheyenne Configuration with a Propeller Blade Solidity of 0.25

$(C_T/\sigma)_{prop} \approx 0.14$. Above this blade loading value, the angles of attack about the propeller disc become large, leading to blade stalling. For the pusher propeller to provide the entire propulsive force during the first part of the manoeuvre, requires an increase of blade solidity.

The solidity of the Cheyenne compound's pusher propeller is increased to 0.25, and the corresponding rotor power, tail-rotor power and pusher propeller power results are shown in Figure **??** (previous page). The results shown in Figure **??** are generally very similar to the results presented in Figure **??**. The only major difference between the results is the change in the required power by the pusher propeller, due to its greater solidity. By increasing the propeller's solidity to 0.25, then it is predicted that the pusher propeller can completely offload the main rotor of its propulsive duties, during the first part of the manoeuvre. This is confirmed by inspecting the blade loading values of the pusher propeller throughout the manoeuvre, as shown in Figure **??**. The increased solidity avoids the pusher propeller reaching the blade stalling limit, which occurs at approximately 0.14. At the 100% case, the maximum power of the pusher propeller reaches 1270 kW, which is greater than the total power required to hover the conventional helicopter at mean sea level. Although the pusher propeller is capable of providing all of the propulsive force to accelerate the aircraft forward, a significant amount of power is required. In low speed flight, the main rotor is clearly more efficient than the pusher propeller in creating propulsive thrust. This result is important for the purposes of designing the flight control system. The compound helicopter is likely to feature a digital fly-by-wire system due to benefits of reducing weight as well as enhancing the handling qualities of the aircraft. For a pilot to fly the Depart and Abort manoeuvre, with minimal workload,

would require an attitude/velocity hold response, as discussed by Fletcher et.al, in the fly-by-wire upgrade to the UH-60 (Ref. **?**). In this mode, a forward stick motion increases airspeed and the pilot is able to hold a constant

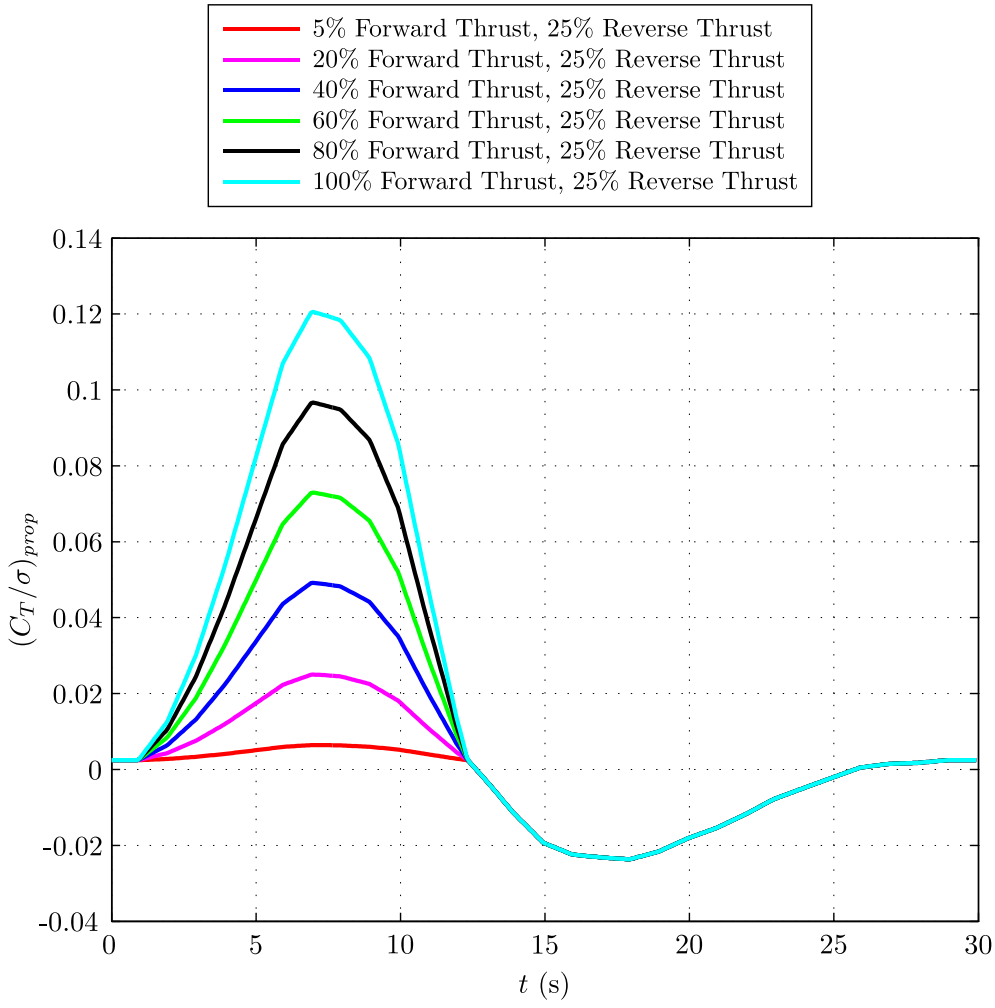

Fig. 20. Total Power Requirements of the Cheyenne Compound with Propeller with a Solidity of 0.25

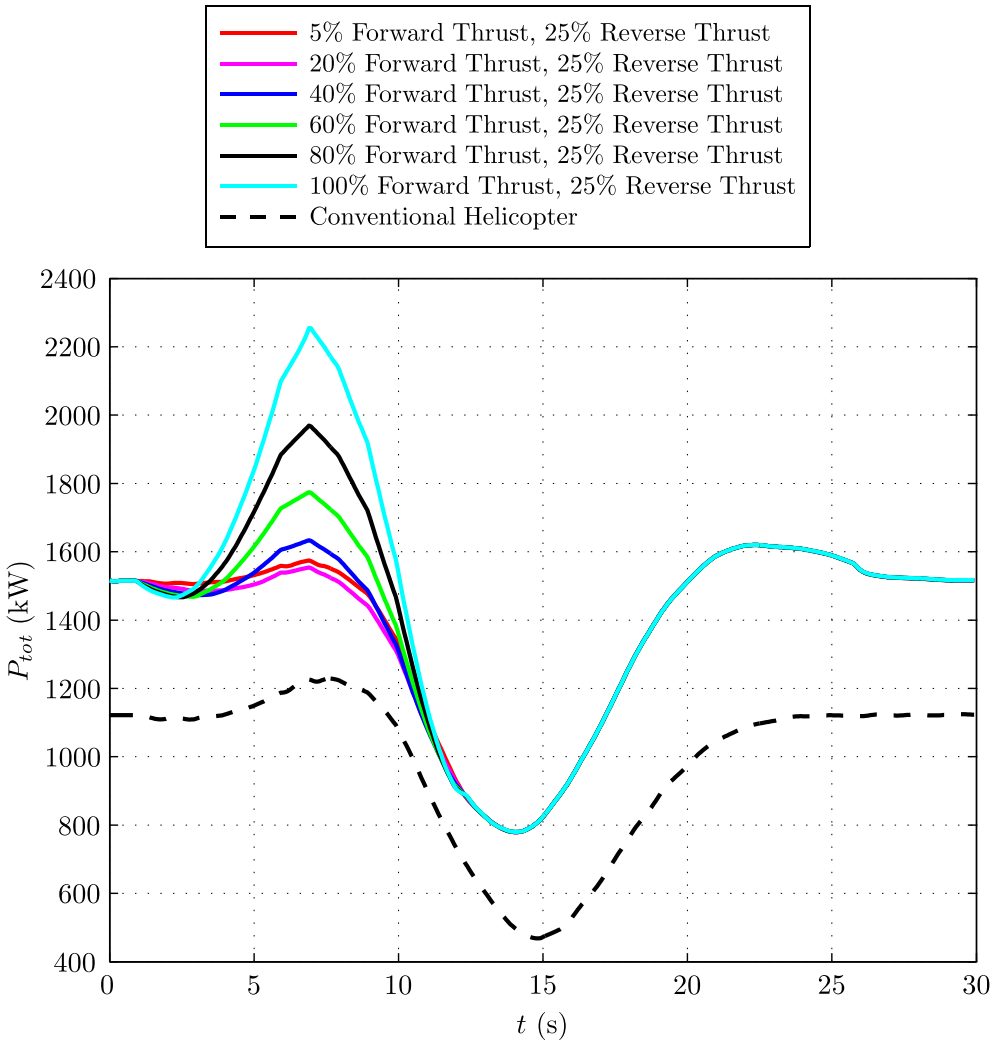

Fig. 21. Total Power Requirements of the Cheyenne Compound with a Propeller Solidity of 0.25

airspeed by re-centring the stick. This control mode would be suitable for the compound helicopter. However, various simulation studies would be required to develop suitable control laws to mix the longitudinal cyclic and propeller pitch controls, so that the vehicle can achieve a smooth acceleration or deceleration by the use of a single control. The results presented in this study show that in low speed flight, the design of the control laws may need to be tailored so that the propeller and the main rotor share the propulsive duties, to avoid flight conditions where the power required is not excessive.

Figure **??** presents the total power required by the Cheyenne configuration, using a propeller solidity of 0.25. Again the results suggest that the Cheyenne compound is able to accelerate forward, from the hover, most efficiently when the main rotor provides the majority of the propulsive thrust. Due to thrust compounding, the pilot of a compound helicopter will have the option to accelerate or decelerate the aircraft by using the propellers or the main rotor. The description of the Depart and Abort test manoeuvre, which will apply to compound helicopters, may have to allow the pilot to fly the manoeuvre in a variety of ways. The first way could be using traditional helicopter manoeuvring, by fully exploiting the main rotor to accelerate and decelerate the aircraft. The second way could involve the pilot sharing the propulsive duties with both the main rotor and the propeller. Lastly, the pilot could fly the manoeuvre with the propeller completely divorcing the main rotor of its propulsive duties. By flying the manoeuvre in a variety of ways, the pilot will be able to check the response of the helicopter for the different control modes. In addition, the pilot will be able to check of the flight control system successfully harmonises the main rotor and propeller controls together.

CONCLUSIONS

The broad aim of this study was to assess the performance of compound helicopters flying the Depart and Abort ADS-33 Mission Task Element. The main conclusions from the paper, are as follows:

1. The propeller design of the compound helicopter is likely to feature highly twisted blades for good propulsive efficiency in forward flight.

2. The level 1 model is capable of predicting the trim control angles of the conventional helicopter, with reasonable accuracy, across the flight envelope. However, a level 2 model is required to accurately predict the main rotor's power requirements in trimmed forward flight.

3. The level 1 is able to successfully predict the pilot controls of the UH-60A helicopter, flying the Depart and Abort MTE.

4. The simulation model predicts the maximum blade loading of the propeller during the Depart and Abort manoeuvre is approximately 0.14.

5. When using a propeller solidity of 0.19 the propeller of the Cheyenne compound helicopter is only capable of providing 85% of the entire total propulsive force during the Depart and Abort manoeuvre.

6. The propeller of the Cheyenne compound helicopter is required to have a solidity of 0.25, so that the propeller can provide the entire total propulsive force during the Depart and Abort manoeuvre.

7. The total power required by the Cheyenne compound helicopter, when flying the Depart and Abort MTE, is minimised when the propeller provides a small portion of the required propulsive thrust. The main rotor is clearly more efficient than the propeller in creating propulsive thrust in low speed flight.

REFERENCES

[1]Hirschberg, M., "Joint Multi-Role Moves Forward," *Vertiflite*, Vol. 60, (1), 2014, pp. 24–26.

[2]Padfield, G., *Helicopter Flight Dynamics: the Theory and Application of Flying Qualities and Simulation Modelling*, Blackwell Publishing, second edition, 2007.

[3]Ferguson, K., "Towards a better understanding of the flight mechanics of compound helicopter configurations," PhD Thesis, University of Glasgow, 2015.

[4]Thomson, D. and Bradley, R., "Inverse simulation as a tool for flight dynamics research - Principles and applications," *Progress in Aerospace Sciences*, Vol. 42, (3), may 2006, pp. 174–210.
doi: 10.1016/j.paerosci.2006.07.002

[5]Rutherford, S., *Simulation Techniques for the Study of the Manoeuvring of Advanced Rotorcraft Configurations*, Ph{.}{d} thesis, University of Glasgow, 1997.

[6]Yeo, H. and Johnson, W., "Optimum Design of a Compound Helicopter," *AIAA Journal of Aircraft*, Vol. 46, (4), 2009.
doi: 10.2514/1.40101

[7]Prouty, R., *Helicopter Performance, Stability, and Control*, Robert E. Krieger Publishing Company, Inc., reprint edition, 1990.

[8]Howlett, J., "UH-60A Black Hawk Engineering Simulation Program: Volume 1 - Mathematical Model," NASA CR-10626, 1984.

[9]Howlett, J., "UH-60A Black Hawk Engineering Simulation Program: Volume 2 - Background Report," NACA CR-166310, 1988.

[10]Orchard, M. and Newman, S., "The fundamental configuration and design of the compound helcopter," *Proceedings of the Institution of Mechanical Engineers, Part G: Journal of Aerospace Engineering*, Vol. 217, (6), 2003, pp. 297–315.
doi: 10.1243/095441003772538570

[11]Keys, C., "Performance Prediction of Helicopters," *Rotary-wing Aerodynamics*, edited by W. Stepniewski, Chap. Volume II, 1979.

[12]Frandenburgh, E. and Segel, R., "Model and full scale compound helicopter research," Helicopter Society 21st Annual, 1965.

[13]Torres, M., "A Wing on the SA.341 Gazelle Helicopter and its Effects," *Vertica*, Vol. 1, (1), 1976, pp. 67–73.

[14]Sipe, O. and Gorenberg, N., "Effect of Mach Number, Reynolds Number and Thickness Ratio on the Aerodynamic Characteristics of NACA 63A-Series Airfoil Sections," USATRECOM TR 65-28, 1965.

[15]Van Dyke, M., "High-Speed Subsonic Characteristics of 16 NACA Six Series Airfoil Sections," NACA TN 2670, 1952.

[16]Adkins, C. and Liebeck, R., "Design of Optimum Propellers," *Journal of Propulsion and Power*, Vol. 10, (5), 1994, pp. 676 – 682.

[17]Wald, Q., "The aerodynamics of propellers," *Progress in Aerospace Sciences*, Vol. 42, (2), 2006, pp. 85–128.
doi: 10.1016/j.paerosci.2006.04.001

[18]Ormiston, R., "Low-Disk Loading Compound Rotorcraft for High-Speed and Aerodynamic Efficiency," International Powered Lift Conference 2010, 2010.

[19]Sforza, P., *Commercial Airplane Design Principles*, Elsevier Aerospace Engineering Series, London, first edition, 2014.

[20]Raymer, D., *Aircraft Design: A Conceptual Approach*, AIAA Education Series, Virginia, fourth edition, 2006.

[21]Marinus, B. and Poppe, J., "Data and design models for military turbo-propeller aircraft," *Aerospace Science and Technology*, Vol. 41, (February), 2015, pp. 63–80.
doi: 10.1016/j.ast.2014.12.009

[22]Hess, R. and Gao, C., "A Generalized Algorithm for Inverse Simulation Applied to Helicopter Maneuvering Flight," *Journal of the American Helicopter Society*, Vol. 38, (4), 1993, pp. 3 – 15.
doi: 10.4050/JAHS.38.3

[23]Thomson, D. and Bradley, R., "Mathematical Definition of Helicopter Maneuvers," *Journal of the American Helicopter Society*, Vol. 4, (1), 1997, pp. 307 – 309.
doi: 10.4050/JAHS.42.307

[24]Hess, R., Gao, C., and Wang, S., "Generalized technique for inverse simulation applied to aircraft maneuvers," *AIAA Journal of Guidance, Control and Dynamics*, Vol. 14, (5), 1991, pp. 920–926.
doi: 10.2514/3.20732

[25]Rutherford, S. and Thomson, D., "Helicopter inverse simulation incorporating an individual blade rotor model," *AIAA Journal of Aircraft*, Vol. 34, (5), 1997.

[26]Blanken, C., Cicolani, L., Sullivan, C., and Arterburn, D., "Evaluation of Aeronautical Design Standard - 33 Using a UH-60A Black Hawk," American Helicopter Society 56th Annual Forum, 2000.

[27]Anon., "Handling qualities requirements for military rotorcraft," Aeronautical design standard ADS-33E-PRF, United States Army Aviation and Troop Command, 2000.

[28]Yeo, H., Bousman, W., and Johnson, W., "Performance analysis of a utility helicopter with standard and advanced rotors," *Journal of the American Helicopter Society*, Vol. 49, (3), 2004, pp. 250–270.
doi: 10.4050/JAHS/49.250

[29]Bousman, W. and Kufeld, R., "UH-60A Airloads Catalog," NASA/TM-2005-212827, 2005.

[30]Bradley, R., Padfield, G., Murray-Smith, D., and Thomson, D., "Validation of helicopter mathematical models," *Transactions of the Institute of Measurement and Control*, Vol. 12, (186), 1990.
doi: 10.1177/014233129001200405

[31]Moodie, A. and Yeo, H., "Design of a Cruise-Efficient Compound Helicopter," *Journal of the American Helicopter Society*, Vol. 57, (3), 2012.
doi: 10.4050/JAHS.57.032004

[32]Fletcher, J., Lusardi, J., Mansur, M., Robinson, D., Arterburn, D., Cherepinsky, I., Driscoll, J., Morse, C., and Kalinowksi, K., "UH-60M Upgrade Fly-By-Wire Flight Control Risk Reduction using the RASCAL JUH-60A In-Flight Simulator," American Helicopter Society 64th Annual Forum, 2008.